

Chapter 24

Variational Methods for Quantum Systems

The variational principle states, that the energy expectation value of any trial function is bounded from below by the exact ground state energy. Therefore, the ground state can be approximated by minimizing the energy of a trial function which involves certain parameters that have to be optimized. In this chapter we study two different kinds of quantum systems. First we apply the variational principle to one- and two-electron systems and calculate the ground state energy of the Helium atom and the Hydrogen molecule. If the trial function treats electron correlation explicitly, the calculation of the energy involves unseparable multidimensional integrals which can be efficiently evaluated with the variational quantum Monte Carlo method. In a second series of computer experiments we study models with a large number of variational parameters. We simulate excitons in a molecular aggregate which are coupled to internal vibrations. The number of parameters increases with the system size up to several hundred and the optimization requires efficient strategies. We use several kinds of trial functions to study the transition from a delocalized to a localized state.

The variational principle is a very valuable tool to approximate the groundstate energy and wavefunction. Consider the representation of the Hamiltonian in a complete basis of eigenfunctions [277]

$$H = \sum_n |\psi_n\rangle E_n \langle \psi_n| \quad (24.1)$$

with the groundstate energy

$$E_0 \leq E_n \quad (24.2)$$

and a trial function with some adjustable parameters

$$\psi_{\text{trial}}(\lambda). \quad (24.3)$$

The expectation value of the Hamiltonian

$$\begin{aligned} \langle \psi_{\text{trial}} | \mathbf{H} \psi_{\text{trial}} \rangle &= \sum_n | \langle \psi_{\text{trial}} | \psi_n \rangle |^2 E_n \geq E_0 \sum_n | \langle \psi_{\text{trial}} | \psi_n \rangle |^2 \\ &= E_0 \langle \psi_{\text{trial}} | \left[\sum_n | \psi_n \rangle \langle \psi_n | \right] \psi_{\text{trial}} \rangle = E_0 | \psi_{\text{trial}} |^2. \end{aligned} \quad (24.4)$$

Hence the energy expectation value is bounded from below by the groundstate energy

$$\frac{\langle \psi_{\text{trial}} | \mathbf{H} \psi_{\text{trial}} \rangle}{| \psi_{\text{trial}} |^2} \geq E_0. \quad (24.5)$$

For the exact groundstate

$$\frac{\langle \psi_0 | \mathbf{H} | \psi_0 \rangle}{| \psi_0 |^2} = E_0$$

and the variance

$$\sigma_E^2 = \frac{\langle \psi_0 | \mathbf{H}^2 | \psi_0 \rangle}{| \psi_0 |^2} - \left(\frac{\langle \psi_0 | \mathbf{H} | \psi_0 \rangle}{| \psi_0 |^2} \right)^2 = 0. \quad (24.6)$$

Now, let us try to find an approximate solution of the eigenvalue problem

$$\mathbf{H} \psi = E_0 \psi \quad (24.7)$$

by optimizing the trial function. The residual is

$$\mathbf{R} = \mathbf{H} \psi_{\text{trial}} - E_0 \psi_{\text{trial}} \quad (24.8)$$

and, applying Galerkin's method (p. 272) we minimize the scalar product

$$\langle \psi_{\text{trial}} | \mathbf{R} \rangle = \langle \psi_{\text{trial}} | \mathbf{H} \psi_{\text{trial}} \rangle - E_0 \langle \psi_{\text{trial}} | \psi_{\text{trial}} \rangle \quad (24.9)$$

where the trial function should be normalized. Alternatively, we divide by the squared norm and minimize

$$\frac{\langle \psi_{\text{trial}} | \mathbf{H} \psi_{\text{trial}} \rangle}{\langle \psi_{\text{trial}} | \psi_{\text{trial}} \rangle} - E_0. \quad (24.10)$$

Hence the "best" trial function is found by minimizing the energy with respect to the parameters λ .

Now, assume that the groundstate is normalized

$$|\psi_0|^2 = 1 \quad (24.11)$$

and choose the normalization of the trial function such that

$$\psi_{trial} = \psi_0 + \rho \quad (24.12)$$

$$\langle \psi_0 | \rho \rangle = 0. \quad (24.13)$$

Then,

$$\frac{\langle \psi_{trial} H \psi_{trial} \rangle}{|\psi_{trial}|^2} = \frac{E_0 + \langle \rho H \rho \rangle}{1 + |\rho|^2} = E_0 + O(|\rho|^2) \quad (24.14)$$

the accuracy of the energy is of second order in $|\rho|$. From

$$\frac{\langle \psi_{trial} H^2 \psi_{trial} \rangle}{|\psi_{trial}|^2} = \frac{E_0^2 + \langle \rho H^2 \rho \rangle}{1 + |\rho|^2} \quad (24.15)$$

we find that the variance of the energy

$$\begin{aligned} \sigma_E^2 &= \frac{\langle \psi_{trial} H^2 \psi_{trial} \rangle}{|\psi_{trial}|^2} - \left(\frac{\langle \psi_{trial} H \psi_{trial} \rangle}{|\psi_{trial}|^2} \right)^2 \\ &= \frac{E_0^2 + \langle \rho H^2 \rho \rangle}{1 + |\rho|^2} - \left(\frac{E_0 + \langle \rho H \rho \rangle}{1 + |\rho|^2} \right)^2 \\ &\approx E_0^2(1 - |\rho|^2) + \langle \rho H^2 \rho \rangle - E_0^2(1 - 2|\rho|^2) - 2E_0 \langle \rho H \rho \rangle \\ &\approx E_0^2 \langle \rho | \rho \rangle^2 + \langle \rho H | H \rho \rangle - 2E_0 \langle \rho H \rho \rangle \\ &\approx |(H - E_0)\rho|^2 \end{aligned} \quad (24.16)$$

is also second order in $|\rho|$. It is bounded from below by zero. Therefore, Quantum Monte Carlo methods often minimize the variance instead of the energy for which the lower bound is unknown.

24.1 Variational Quantum Monte Carlo Simulation of Atomic and Molecular Systems

Electron structure calculations for atoms and molecules beyond the self consistent field level (Hartree Fock uses one Slater determinant as a trial function, MCSCF methods a combination of several) need an explicit treatment of electron correlation. This can be achieved by expanding the wavefunction into a large number of

configurations (CI method) or, alternatively, by using trial functions which depend explicitly on the electron-electron distances. Very popular [332, 333] are factors of the Jastrow pair-correlation [334] type

$$\exp \left\{ \sum_{i < j} U(r_{ij}) \right\} \quad (24.17)$$

where in the simplest case

$$U(r_{ij}) = \frac{\alpha r_{ij}}{1 + \beta r_{ij}} \quad (24.18)$$

has the form of a Pade approximant. Wavefunctions including a Jastrow factor do not factorize and make it necessary to apply Monte Carlo integration methods to calculate the energy expectation value (see p. 205). For the computer simulation of two-electron systems we use trial functions of the type

$$\psi = e^{-\kappa r_{1a}} e^{-\kappa r_{2b}} e^{\alpha r_{12}/(1+\beta r_{12})} \quad (24.19)$$

which are products of two 1s-orbitals centered at the (possibly same) positions $\mathbf{r}_{a,b}$ and a Jastrow factor. In the following, we abbreviate

$$u = 1 + \beta r_{12}. \quad (24.20)$$

Starting with the derivatives

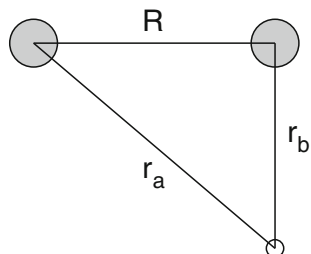
$$\frac{\partial}{\partial x_1} \psi = -\frac{\kappa x_{1a}}{r_{1a}} \psi + \frac{\alpha x_{12}}{r_{12} u^2} \psi \quad (24.21)$$

$$\begin{aligned} \frac{\partial^2}{\partial x_1^2} \psi &= \left[-\frac{\kappa x_{1a}}{r_{1a}} + \frac{\alpha x_{12}}{r_{12} u^2} \right]^2 \psi \\ &+ \left[-\frac{\kappa}{r_{1a}} + \frac{\kappa x_{1a}^2}{r_{1a}^3} \right] \psi + \left[\frac{\alpha}{r_{12} u^2} - \frac{\alpha x_{12}^2}{r_{12}^3 u^2} - 2 \frac{\alpha \beta x_{12}^2}{r_{12}^2 u^3} \right] \psi \end{aligned} \quad (24.22)$$

we calculate the kinetic energy

$$\begin{aligned} T\psi &= -\frac{1}{2}(\nabla_1^2 + \nabla_2^2)\psi = \left[-\kappa^2 - \frac{\alpha^2}{u^4} + \frac{\alpha\kappa}{u^2} \left(\frac{\mathbf{r}_{1a}}{r_{1a}} - \frac{\mathbf{r}_{2b}}{r_{2b}} \right) \frac{\mathbf{r}_{12}}{r_{12}} \right] \psi \\ &+ \left[\frac{\kappa}{r_{1a}} + \frac{\kappa}{r_{2b}} - \frac{2\alpha}{r_{12} u^2} + 2 \frac{\alpha\beta}{u^3} \right] \psi. \end{aligned} \quad (24.23)$$

For short electron-electron distance

Fig. 24.1 Geometry of H_2^+ 

$$T\psi \rightarrow \left[-\kappa^2 - \alpha^2 + \alpha\kappa \left(\frac{\mathbf{r}_{1a}}{r_{1a}} - \frac{\mathbf{r}_{2b}}{r_{2b}} \right) \frac{\mathbf{r}_{12}}{r_{12}} + \frac{\kappa}{r_{1a}} + \frac{\kappa}{r_{2b}} + 2\alpha\beta - \frac{2\alpha}{r_{12}} \right] \psi. \quad (24.24)$$

A choice of $\alpha = 1/2$ cancels the divergent Coulomb repulsion at $r_{12} \rightarrow 0$ and fulfills the electron-electron cusp condition [333, 335]. More complicated Jastrow factors also allow to fulfill the electron-nuclei cusp conditions.

24.1.1 The Simplest Molecule: H_2^+

As a first example (Problem 24.1), we consider an electron moving in the Coulomb field of two protons (Fig. 24.1). Applying the Born-Oppenheimer approximation the protons are kept fixed at a distance R . In atomic units,¹ the Hamiltonian is

$$H = T + V = -\frac{1}{2}\nabla^2 - \frac{1}{r_a} - \frac{1}{r_b} + \frac{1}{R}. \quad (24.25)$$

This eigenvalue problem can be solved exactly (using elliptic coordinates) and is also a popular example for the variational method.

As a trial wavefunction we use the linear combination of two hydrogen-like 1s orbitals

$$\varphi_a = \sqrt{\frac{\kappa^3}{\pi}} e^{-\kappa r_a} \quad \varphi_b = \sqrt{\frac{\kappa^3}{\pi}} e^{-\kappa r_b} \quad (24.26)$$

which are solutions for the problem with two nuclear charges κ at infinite distance. At finite distances, the variational parameter κ is a measure of the effective nuclear charge. For large distance $\kappa = 1$ as for a single proton whereas at short distances the optimum value approaches $\kappa = 2$ as for the He^+ ion.

Since the problem is highly symmetric, we take a symmetric combination

¹i.e. setting $a_B = 4\pi\epsilon_0\hbar^2/e^2m_e = 1$ and $\hbar^2/m_e = 1$.

$$\varphi_{\text{trial}} = \frac{1}{\sqrt{2(1 \pm S)}} [\varphi_a \pm \varphi_b] \quad (24.27)$$

where the overlap integral can be calculated using elliptic coordinates

$$\begin{aligned} r_a &= \frac{R}{2}(\lambda + \mu) & r_b &= \frac{R}{2}(\lambda - \mu) \\ S &= \int \int \int \varphi_a \varphi_b dV = 2\pi \int_1^\infty d\lambda \int_{-1}^1 d\mu \, 2\kappa^3 (\lambda^2 - \mu^2) \frac{R^3}{8} e^{-\kappa R \lambda} \\ &= e^{-\kappa R} \left(1 + \kappa R + \frac{\kappa^2 R^2}{3} \right). \end{aligned} \quad (24.28)$$

The action of the Hamiltonian is

$$H\varphi_a = -\frac{1}{2} \left(\kappa^2 - \frac{2\kappa}{r_a} \right) \varphi_a + \left[\frac{1}{R} - \frac{1}{r_a} - \frac{1}{r_b} \right] \varphi_a = \left[-\frac{1}{r_b} + \frac{\kappa - 1}{r_a} + \left(-\frac{\kappa^2}{2} + \frac{1}{R} \right) \right] \varphi_a \quad (24.29)$$

$$H\varphi_b = -\frac{1}{2} \left(\kappa^2 - \frac{2\kappa}{r_b} \right) \varphi_b + \left[\frac{1}{R} - \frac{1}{r_a} - \frac{1}{r_b} \right] \varphi_b = \left[-\frac{1}{r_a} + \frac{\kappa - 1}{r_b} + \left(-\frac{\kappa^2}{2} + \frac{1}{R} \right) \right] \varphi_b \quad (24.30)$$

$$H\varphi_{\text{trial}} = \frac{1}{\sqrt{2(1 \pm S)}} \left[\left(\frac{\kappa}{r_a} - \frac{\kappa^2}{2} \right) \varphi_a \pm \left(\frac{\kappa}{r_b} - \frac{\kappa^2}{2} \right) \varphi_b \right] + \left[\frac{1}{R} - \frac{1}{r_a} - \frac{1}{r_b} \right] \varphi_{\text{trial}}$$

from which we obtain the local energy

$$E_{\text{loc}} = \left[\frac{1}{R} - \frac{1}{r_a} - \frac{1}{r_b} - \frac{\kappa^2}{2} \right] + \frac{\frac{\kappa}{r_a} \varphi_a \pm \frac{\kappa}{r_b} \varphi_b}{\varphi_a \pm \varphi_b}. \quad (24.31)$$

For comparison, we calculate the expectation value of the energy

$$\langle \varphi_{\text{trial}} H \varphi_{\text{trial}} \rangle = \frac{1}{2(1 \pm S)} [H_{aa} + H_{bb} \pm H_{ab} \pm H_{ba}] = \frac{H_{aa} \pm H_{ab}}{1 \pm S} \quad (24.32)$$

with the matrix elements

$$H_{aa} = H_{bb} = \frac{1}{R} - \frac{\kappa^2}{2} - \int \frac{\varphi_a^2}{r_b} dV + (\kappa - 1) \int \frac{\varphi_a^2}{r_a} dV \quad (24.33)$$

$$H_{ab} = H_{ba} = \left(\frac{1}{R} - \frac{\kappa^2}{2} \right) S - \int \frac{\varphi_a \varphi_b}{r_a} dV + (\kappa - 1) \int \frac{\varphi_a \varphi_b}{r_b} dV. \quad (24.34)$$

The integrals can be evaluated in elliptic coordinates

$$\int \frac{\varphi_b^2}{r_b} dV = \int \frac{\varphi_a^2}{r_a} dV = 2\kappa^3 \int_1^\infty d\lambda \int_{-1}^1 d\mu \frac{R^2}{4} (\lambda - \mu) e^{-\kappa R(\lambda + \mu)/2} = \kappa \quad (24.35)$$

$$\begin{aligned} \int \frac{\varphi_b^2}{r_a} dV &= \int \frac{\varphi_a^2}{r_b} dV = 2\kappa^3 \int_1^\infty d\lambda \int_{-1}^1 d\mu \frac{R^2}{4} (\lambda + \mu) e^{-\kappa R(\lambda + \mu)/2} \\ &= \frac{1}{R} - e^{-2\kappa R} \left(\kappa + \frac{1}{R} \right) \end{aligned} \quad (24.36)$$

$$\begin{aligned} \int \frac{\varphi_a \varphi_b}{r_b} dV &= \int \frac{\varphi_a \varphi_b}{r_a} dV = 2\kappa^3 \int_1^\infty d\lambda \int_{-1}^1 d\mu \frac{R^2}{4} (\lambda - \mu) e^{-\kappa R\lambda} \\ &= e^{-\kappa R} \left(\kappa + \kappa^2 R \right). \end{aligned} \quad (24.37)$$

In our computer experiment (Problem 24.1), we first keep $\kappa = 1$ fixed and use the variational MC method to calculate the expectation value of the energy. Figure 24.2 compares the results with the exact value (24.32). Next we vary κ and determine the optimum value at each point R by minimizing $E(R, \kappa)$. Figure 24.3 shows the κ -dependence for several points. The optimized κ -values (Fig. 24.4) lead to lower energies, especially at short distances. The equilibrium is now at $R_0 = 2.0$ Bohr with a minimum energy of -0.587 a.u. instead of 2.5 Bohr and -0.565 a.u. for $\kappa = 1$. (Exact values are 2.00 Bohr and -0.603 a.u. [277]).

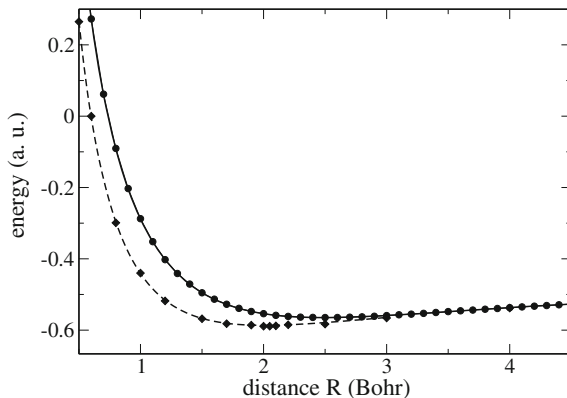


Fig. 24.2 (Adiabatic groundstate energy of H_2^+) The potential energy curve of H_2^+ is calculated with the variational method. *Circles* show the results from MC integration for a maximum step length of 0.5 Bohr and averages over 2×10^7 samples for a fixed effective charge $\kappa = 1$. The *solid curve* shows the results of the exact integration (24.32) for comparison. *Diamonds* show the MC results after optimizing $\kappa(R)$ at each point. The *dashed curve* shows the results of the exact integration (24.32) where $\kappa(R)$ was determined by solving $\frac{\partial}{\partial \kappa} \langle \varphi_{\text{trial}} | H | \varphi_{\text{trial}} \rangle = 0$ numerically

Fig. 24.3 (Optimization of the variational parameter κ for H_2^+) The groundstate energy from MC integration is shown as a function of κ for $R = 1$ (diamonds), $R = 2$ (squares) and $R = 3$ (circles). The curves show a fit with a cubic polynomial which helps to find the minima

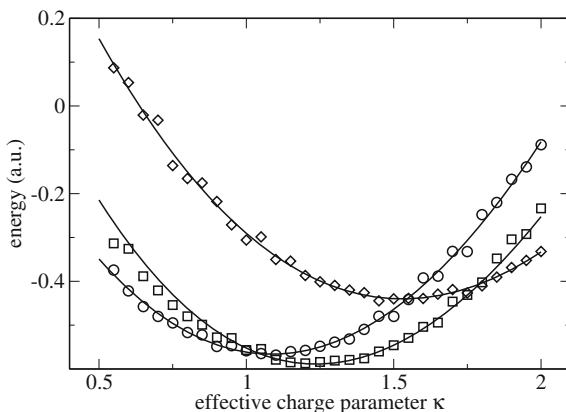


Fig. 24.4 (Optimized effective charge parameter for H_2^+) The variational parameter κ is optimized by minimizing the MC energy as shown in Fig. 24.3 (circles). The curve shows the exact values obtained by minimizing (24.32) numerically

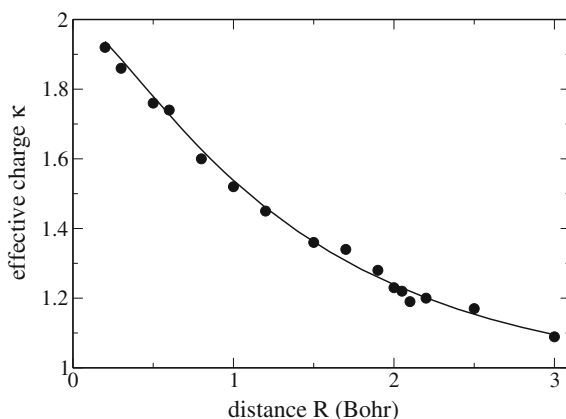
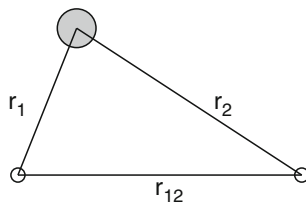


Fig. 24.5 Geometry of He



24.1.2 The Simplest Two-Electron System: The Helium Atom

The Helium atom (Fig. 24.5) is the simplest “many-electron” system where electron-electron interaction has to be taken into account. The electronic Hamiltonian reads in atomic units

$$H = -\frac{1}{2}\nabla_1^2 - \frac{1}{2}\nabla_2^2 - \frac{2}{r_1} - \frac{2}{r_2} + \frac{1}{r_{12}}. \quad (24.38)$$

Without electron-electron interaction, the singlet groundstate would be simply given in terms of hydrogen-like 1s-orbitals as

$$\psi_0 = \frac{2^3}{\pi} e^{-2r_1} e^{-2r_2} \frac{1}{\sqrt{2}} (\uparrow(1) \downarrow(2) - \uparrow(2) \downarrow(1)) \quad (24.39)$$

with

$$\left[-\frac{1}{2} \nabla_1^2 - \frac{1}{2} \nabla_2^2 - \frac{2}{r_1} - \frac{2}{r_2} \right] \psi_0 = -2 \left(1 - \frac{1}{r_1} \right) \psi_0 - 2 \left(1 - \frac{1}{r_2} \right) \psi_0 - \frac{2}{r_1} \psi_0 - \frac{2}{r_2} \psi_0 = -4\psi_0. \quad (24.40)$$

For the variational treatment (Problem 24.2) we use a trial wavefunction with a variable exponent to take the partial shielding of the central charge into account

$$\psi_{trial} = \frac{\kappa^3}{\pi} e^{-\kappa r_1} e^{-\kappa r_2} \frac{1}{\sqrt{2}} (\uparrow(1) \downarrow(2) - \uparrow(2) \downarrow(1)) \quad (24.41)$$

where the antisymmetric spin function accounts for the Pauli principle.

Then,

$$H\psi_{trial} = -\frac{1}{2} \left(\kappa^2 - \frac{2\kappa}{r_1} + \kappa^2 - \frac{2\kappa}{r_2} \right) \psi_{trial} + \left(\frac{1}{r_{12}} - \frac{2}{r_1} - \frac{2}{r_2} \right) \psi_{trial} \quad (24.42)$$

$$E_{loc} = \frac{1}{r_{12}} - \kappa^2 + \frac{\kappa - 2}{r_1} + \frac{\kappa - 2}{r_2}. \quad (24.43)$$

The integration can be performed analytically [277]. First we calculate

$$\left(\frac{\kappa^3}{\pi} \right)^2 \int e^{-2\kappa r_1} e^{-2\kappa r_2} \frac{1}{r_1} dV_1 dV_2 = \frac{\kappa^3}{\pi} \int e^{-2\kappa r} \frac{1}{r} dV = \kappa. \quad (24.44)$$

The integral of the electron-electron interaction is

$$\begin{aligned} & \left(\frac{\kappa^3}{\pi} \right)^2 \int e^{-2\kappa r_1} e^{-2\kappa r_2} \frac{1}{r_{12}} dV_1 dV_2 \\ &= \left(\frac{\kappa^3}{\pi} \right)^2 \int_0^\infty r_1^2 dr_1 e^{-2\kappa r_1} \int_0^\infty r_2^2 dr_2 e^{-2\kappa r_2} \int d\Omega_1 \int d\Omega_2 \frac{1}{r_{12}} \\ &= \left(\frac{\kappa^3}{\pi} \right)^2 \int_0^\infty r_1^2 dr_1 e^{-2\kappa r_1} \int_0^\infty r_2^2 dr_2 e^{-2\kappa r_2} \frac{(4\pi)^2}{\max(r_1, r_2)} \end{aligned}$$

$$\begin{aligned}
&= \left(\frac{\kappa^3}{\pi}\right)^2 \int_0^\infty r_1^2 dr_1 e^{-2\kappa r_1} (4\pi)^2 \left[\frac{1}{r_1} \int_0^{r_1} r_2^2 dr_2 e^{-2\kappa r_2} + \int_{r_1}^\infty r_2 dr_2 e^{-2\kappa r_2} \right] \\
&= 16\kappa^6 \int_0^\infty r_1^2 dr_1 e^{-2\kappa r_1} \left[\frac{1 - e^{-2\kappa r_1}}{4r_1\kappa^3} - \frac{e^{-2\kappa r_1}}{4\kappa^2} \right] \\
&= \frac{5}{8}\kappa.
\end{aligned} \tag{24.45}$$

Together, we obtain

$$\langle \psi_{\text{trial}} | H | \psi_{\text{trial}} \rangle = -\kappa^2 + \frac{5}{8}\kappa + 2(\kappa - 2)\kappa = \kappa^2 + \left(\frac{5}{8} - 4\right)\kappa \tag{24.46}$$

which has its minimum at (Figs. 24.6 and 24.7)

$$\kappa_{\text{min}} = 2 - \frac{5}{16} \approx 1.688 \tag{24.47}$$

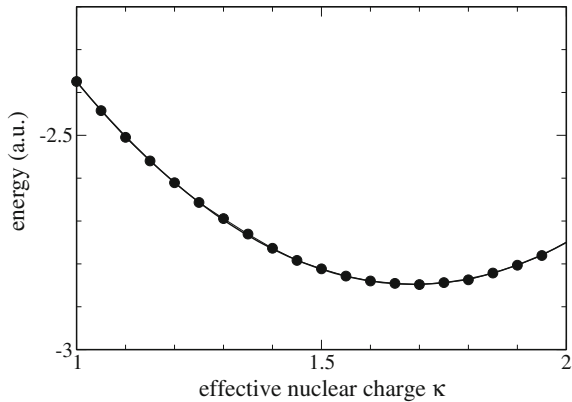
with the value

$$\min_{\kappa} \langle \psi_{\text{trial}} | H | \psi_{\text{trial}} \rangle = -\frac{729}{256} \approx -2.848.$$

Next, we consider a (not normalized) trial wavefunction of the Slater-Jastrow type (24.19)

$$\psi_{\text{trial}} = e^{-\kappa r_1} e^{-\kappa r_2} e^{\alpha r_{12}/(1+\beta r_{12})} \frac{1}{\sqrt{2}} (\uparrow(1)\downarrow(2) - \uparrow(2)\downarrow(1)). \tag{24.48}$$

Fig. 24.6 (Optimization of the effective charge for the Helium atom) The groundstate energy of the Helium atom was calculated with MC integration. The circles show the average over 10^7 points. The curve shows the exact result (24.46) for comparison. The optimum value is $\kappa = 1.688$



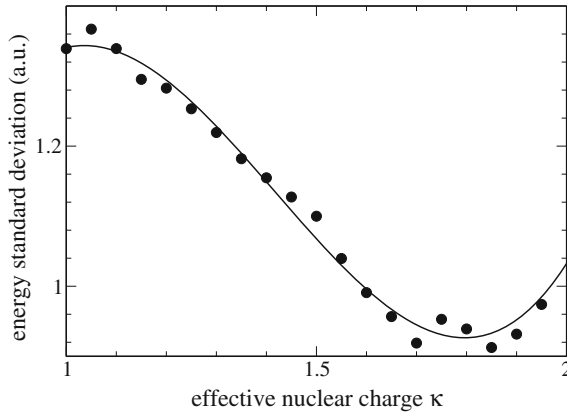


Fig. 24.7 (Standard deviation of the MC energy) The *Circles* show the standard deviation of the MC energy for Helium. Its minimum between $\kappa = 1.7 \dots 1.9$ is close to the minimum of the energy (Fig. 24.6). The *curve* shows a cubic polynomial fit

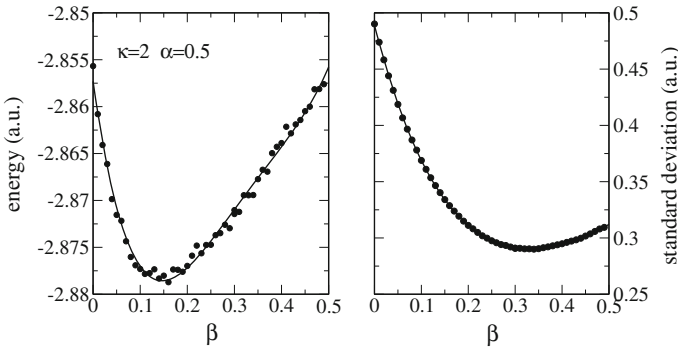


Fig. 24.8 (Variation of β) The groundstate of the Helium atom is approximated with the Slater-Jastrow wavefunction (24.48). Singularities of the potential energy are removed by using $\kappa = 2$ and $\alpha = 1/2$. Each point represents an average over 10^7 samples. *Left* The energy minimum of -2.879 is found at $\beta = 0.15$. *Right* the standard deviation has a minimum value of 0.29 at $\beta = 0.35$

From (24.23) with $\mathbf{r}_a = \mathbf{r}_b$ we find the local energy

$$E_{loc} = \frac{\kappa - 2}{r_1} + \frac{\kappa - 2}{r_2} + \frac{1}{r_{12}} \left(1 - \frac{2\alpha}{u^2} \right) + \frac{2\alpha\beta}{u^3} - \kappa^2 - \frac{\alpha^2}{u^4} + \frac{\kappa\alpha}{u^2} \left(\frac{\mathbf{r}_1}{r_1} - \frac{\mathbf{r}_2}{r_2} \right) \cdot \frac{(\mathbf{r}_1 - \mathbf{r}_2)}{r_{12}}. \tag{24.49}$$

With fixed values $\alpha = 1/2$ and $\kappa = 2$ all singularities in the local energy are removed, but this also reduces the flexibility of the test function. The energy minimum of -2.879 is found at $\beta = 0.15$ (Fig. 24.8). A further improvement can be achieved by varying the exponent κ together with β . The minimum now is -2.885 at $\kappa = 1.91$ (Fig. 24.9). If we drop the cusp condition and vary all three parameters we find a

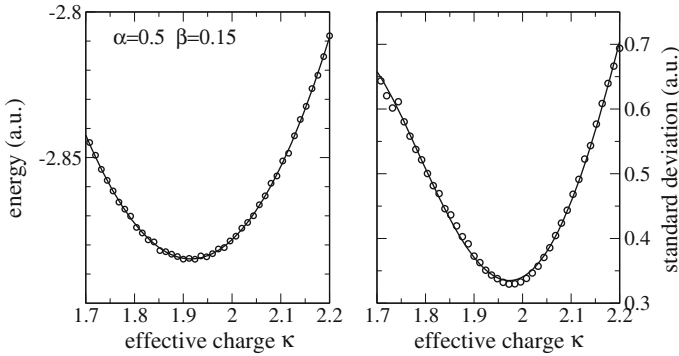


Fig. 24.9 (Variation of κ) The groundstate of the Helium atom is approximated with the Slater-Jastrow wavefunction (24.48). From Fig. 24.8 the optimized value of $\beta = 0.15$ is taken, $\alpha = 1/2$. Each point represents an average over 10^7 samples. **Left** The energy minimum of -2.885 is found at $\kappa = 1.91$. **Right** the standard deviation has a minimum value of 0.33 at $\kappa = 1.98$

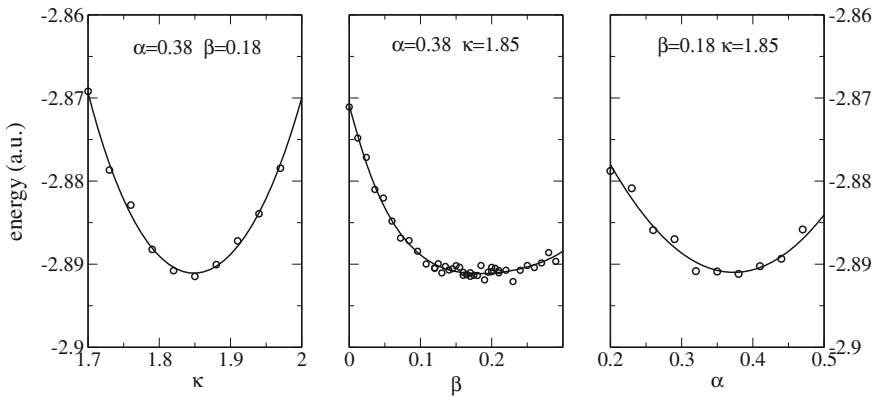


Fig. 24.10 (Variation of all parameters) The groundstate of the Helium atom is approximated with the Slater-Jastrow wavefunction (24.48). Variation of all three parameters gives a lowest energy of -2.891 for $\alpha = 0.38$, $\beta = 0.18$, $\kappa = 1.85$

slightly smaller value of -2.891 with a standard variation of $\sigma = 0.36$ (Fig. 24.10). More sophisticated trial wavefunctions reproduce the exact value of -2.903724 even more accurately [336, 337].

24.1.3 The Hydrogen Molecule H_2

The Helium atom can be considered as the limiting case of the H_2 molecule for zero distance (neglecting nuclear Coulomb repulsion). At finite distance R the one-

electron factors of the wavefunction have to be symmetrized.² We use a trial function (we omit the singlet spin function and do not normalize the wavefunction)

$$\begin{aligned}\psi &= C [\varphi_a(r_1)\varphi_b(r_2) + \varphi_b(r_1)\varphi_a(r_2)] + (1 - C) [\varphi_a(r_1)\varphi_a(r_2) + \varphi_b(r_1)\varphi_b(r_2)] \\ &= C\psi_{VB} + (1 - C)\psi_{ionic}\end{aligned}\quad (24.50)$$

which combines covalent and ionic configurations

$$\psi_{VB} = (\varphi_a(r_1)\varphi_b(r_2) + \varphi_b(r_1)\varphi_a(r_2)) \quad (24.51)$$

$$\psi_{ionic} = (\varphi_a(r_1)\varphi_a(r_2) + \varphi_b(r_1)\varphi_b(r_2)) \quad (24.52)$$

and includes as special cases

- the Heitler-London or valence-bond ansatz ($C = 1$) ψ_{VB}
- the Hund-Mulliken-Bloch or molecular orbital method where the symmetric MO is doubly occupied ($C = 0.5$)

$$\begin{aligned}\psi_{MO}^{++} &= (\varphi_a(r_1) + \varphi_b(r_1)) (\varphi_a(r_2) + \varphi_b(r_2)) \\ &= \psi_{VB} + \psi_{ionic}\end{aligned}\quad (24.53)$$

- the Heitler-London method augmented by ionic contributions $C = (1 + \lambda)^{-1}$

$$\psi = \psi_{VB} + \lambda\psi_{ionic} \quad (24.54)$$

- the MCSCF ansatz which mixes two determinants ($C = 1 - C_d$)

$$\begin{aligned}\psi &= \psi_{MO}^{++} + C_d\psi_{MO}^{--} \\ &= (\varphi_a(r_1) + \varphi_b(r_1)) (\varphi_a(r_2) + \varphi_b(r_2)) + C_d (\varphi_a(r_1) - \varphi_b(r_1)) (\varphi_a(r_2) - \varphi_b(r_2)) \\ &= (1 - C_d)\psi_{VB} + (1 + C_d)\psi_{ionic}.\end{aligned}\quad (24.55)$$

The molecular orbital method corresponds to the Hartree–Fock method which is very popular in molecular physics. At large distance it fails to describe two separate hydrogen atoms with an energy of -1 au properly. In the bonding region it is close to the valence bond method which has the proper asymptotic limit. Both predict an equilibrium around $R = 1.6$ (Fig. 24.11).

To improve the results we vary the effective charge κ and the configuration mixing C (Fig. 24.12). Optimization of κ lowers the energy especially at small internuclear distances where the effective charge reaches a value of 2 as for the Helium atom (Fig. 24.13). The minimum of the potential curve now is found at a much more reasonable value of $R = 1.4$. Variation of the configuration mixing lowers the energy

²We consider only singlet states with antisymmetric spin part.

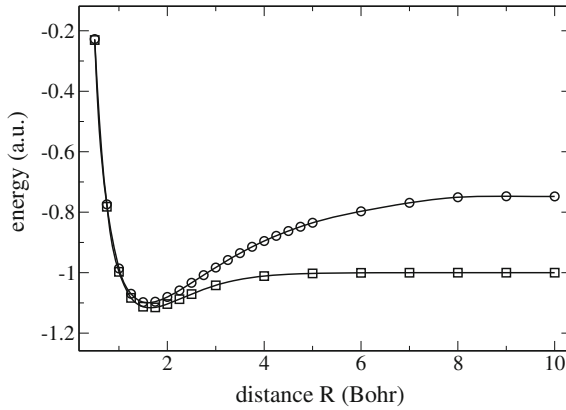


Fig. 24.11 (Comparison of Heitler-London and Hund-Mulliken-Bloch energies for H_2) The MO method (*circles*) fails to describe the asymptotic behaviour at large distances properly. In the bonding region it is close to the VB method (*squares*). Both predict a minimum around $R = 1.6$

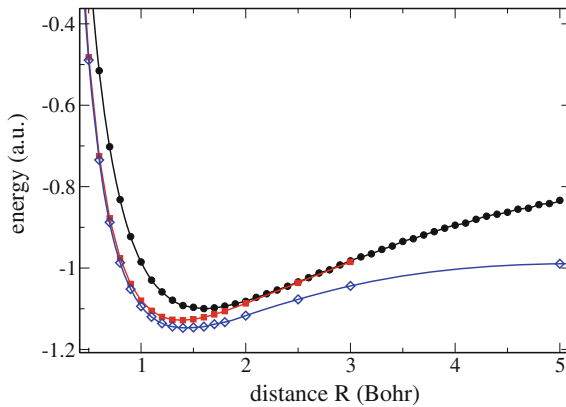


Fig. 24.12 (Optimization of effective charge κ and configuration mixing C) Starting from the MO energy (*black circles*) optimization of κ (*red squares*) and C (*blue diamonds*) lower the energy considerably and shift the potential minimum from 1.6 to 1.4 Bohr (see Problem 24.3)

mostly at larger distances where the proper limit is now obtained. For our computer experiment (Problem 24.3) we include a Jastrow factor into the trial function

$$\psi = \left\{ C \left[e^{-\kappa r_{1a} - \kappa r_{2b}} + e^{-\kappa r_{1b} - \kappa r_{2a}} \right] + (1 - C) \left[e^{-\kappa r_{1a} - \kappa r_{2a}} + e^{-\kappa r_{1b} - \kappa r_{2b}} \right] \right\} \times \exp \left\{ \frac{\alpha r_{12}}{1 + \beta r_{12}} \right\} \quad (24.56)$$

and vary κ , β and C to minimize the expectation value of the local energy

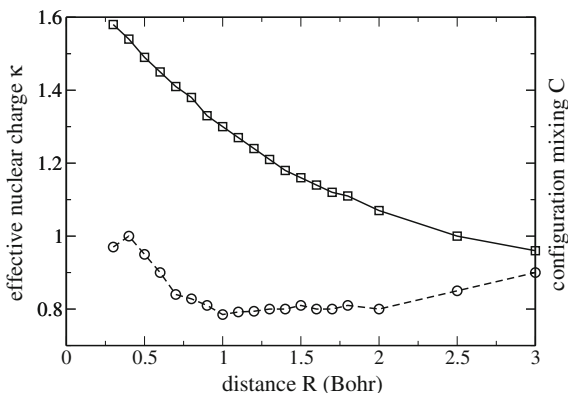


Fig. 24.13 (Optimized values of κ and C) The effective charge (*squares*) approaches $\kappa = 2$ at very short distances corresponding to the He atom. Configuration mixing (*circles*) is most important in the bonding region. At large distances the valence bond wavefunction ($C = 1$) provides the lowest energy. At very small distances the two configurations become equivalent making the mixing meaningless as $R \rightarrow 0$

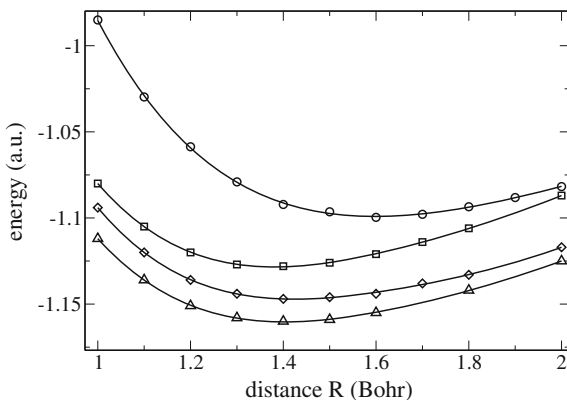
$$\begin{aligned}
 E_{loc} = & \frac{1}{r_{12}} \left(1 - \frac{2\alpha}{u^2} \right) - \frac{1}{r_{1a}} - \frac{1}{r_{1b}} - \frac{1}{r_{2a}} - \frac{1}{r_{2b}} + \frac{2\alpha\beta}{u^3} - \kappa^2 - \frac{\alpha^2}{u^4} \\
 & + C \left[\frac{\kappa}{r_{1a}} + \frac{\kappa}{r_{2b}} + \frac{\kappa\alpha}{u^2} \left(\frac{\mathbf{r}_{1a}}{r_{1a}} - \frac{\mathbf{r}_{2b}}{r_{2b}} \right) \frac{(\mathbf{r}_1 - \mathbf{r}_2)}{r_{12}} \right] e^{\alpha r_{12}/u - \kappa r_{1a} - \kappa r_{2b}} \psi^{-1} \\
 & + C \left[\frac{\kappa}{r_{1b}} + \frac{\kappa}{r_{2a}} + \frac{\kappa\alpha}{u^2} \left(\frac{\mathbf{r}_{1b}}{r_{1b}} - \frac{\mathbf{r}_{2a}}{r_{2a}} \right) \frac{(\mathbf{r}_1 - \mathbf{r}_2)}{r_{12}} \right] e^{\alpha r_{12}/u - \kappa r_{1b} - \kappa r_{2a}} \psi^{-1} \\
 & + (1 - C) \left[\frac{\kappa}{r_{1a}} + \frac{\kappa}{r_{2a}} + \frac{\kappa\alpha}{u^2} \left(\frac{\mathbf{r}_{1a}}{r_{1a}} - \frac{\mathbf{r}_{2a}}{r_{2a}} \right) \frac{(\mathbf{r}_1 - \mathbf{r}_2)}{r_{12}} \right] e^{\alpha r_{12}/u - \kappa r_{1a} - \kappa r_{2a}} \psi^{-1} \\
 & + (1 - C) \left[\frac{\kappa}{r_{1b}} + \frac{\kappa}{r_{2b}} + \frac{\kappa\alpha}{u^2} \left(\frac{\mathbf{r}_{1b}}{r_{1b}} - \frac{\mathbf{r}_{2b}}{r_{2b}} \right) \frac{(\mathbf{r}_1 - \mathbf{r}_2)}{r_{12}} \right] e^{\alpha r_{12}/u - \kappa r_{1b} - \kappa r_{2b}} \psi^{-1}.
 \end{aligned} \tag{24.57}$$

In the bonding region the energy is lowered by further 0.01 au with a minimum value of -1.16 au (Fig. 24.14). This effect is small as part of the correlation is already included in the two-determinant ansatz. More sophisticated trial functions or larger CI expansions give -1.174 a.u. quite close to the exact value [333].

24.2 Exciton-Phonon Coupling in Molecular Aggregates

In this section we simulate excitons in a molecular aggregate which are coupled to internal vibrations of the molecular units. Molecular aggregates are of considerable interest for energy transfer in artificial [338] and biological systems [339]. Even

Fig. 24.14 (Optimization of the Slater-Jastrow wavefunction for H_2) Optimization of the Jastrow factor lowers the energy by further 0.01 au (triangles). Circles show the MO energy, squares the MO energy with optimized exponent κ and diamonds the optimized MCSCF energies as in Fig. 24.13



simple trial functions involve a large number of parameters which have to be optimized and require efficient strategies to minimize the energy. We consider a finite periodic system like in the light harvesting complex of photosynthesis. An optical excitation on the n -th molecule is denoted by the state $|n\rangle$. It can be transferred to the neighboring molecules by the excitonic coupling V and is coupled to the vibrational coordinate q_n . (For simplicity, we consider only one internal vibration per molecule). The model Hamiltonian reads in dimensionless units (periodic b.c. imply that $|0\rangle \equiv |N\rangle$ and $|N+1\rangle \equiv |1\rangle$)

$$\begin{aligned}
 H &= \sum_{mm} |m\rangle H_{mn} \langle n| \\
 &= \frac{\lambda^2}{2} + \sum_n \left(-\frac{1}{2} \frac{\partial^2}{\partial q_n^2} + \frac{1}{2} q_n^2 \right) + \sum_{n=1}^N |n\rangle \lambda q_n \langle n| + |n\rangle V \langle n+1| + |n\rangle V \langle n-1|.
 \end{aligned}
 \tag{24.58}$$

Due to the N -fold degeneracy of the excited states, a simple Born-Oppenheimer wavefunction is not adequate. Instead we consider a sum of N Born-Oppenheimer products

$$\Psi = \sum_n |n\rangle \Phi_n(q_1, \dots, q_N).
 \tag{24.59}$$

We use the variational principle to approximate the lowest eigenstate. Obviously, the number of variational parameters will rapidly increase with the system size. Even if we introduce only one parameter for each unit, e.g. a shift of the potential minimum, this requires N^2 parameters for the aggregate.

The Hamiltonian (24.58) can be brought to a more convenient form by a unitary transformation with

$$S = \sum_n |n \rangle G^n \langle n| \quad (24.60)$$

where the translation operator G transforms the nuclear coordinates according to

$$Gq_nG^{-1} = q_{n+1}. \quad (24.61)$$

The transformed Hamiltonian then reads

$$= \frac{\lambda^2}{2} + \sum_n \left(-\frac{1}{2} \frac{\partial^2}{\partial q_n^2} + \frac{1}{2} q_n^2 \right) + \lambda q_0 + |n \rangle VG \langle n+1| + |n \rangle VG^{-1} \langle n-1|. \quad (24.62)$$

Delocalized exciton states

$$|k \rangle = \frac{1}{\sqrt{N}} \sum_n e^{ikn} |n \rangle \quad (24.63)$$

transform the Hamiltonian into N independent exciton modes

$$\tilde{H} = \sum_k |k \rangle H_k \langle k| \quad (24.64)$$

with

$$H_k = \frac{\lambda^2}{2} + \sum_n \left(-\frac{1}{2} \frac{\partial^2}{\partial q_n^2} + \frac{1}{2} q_n^2 \right) + \lambda q_0 + V e^{ik} G + V e^{-ik} G^{-1}. \quad (24.65)$$

Hence, we conclude that the eigenfunctions of the Hamiltonian H have the general form

$$\Psi = \frac{1}{\sqrt{N}} \sum_n e^{ikn} |n \rangle G^n \Phi_k$$

where Φ_k is an eigenfunction of H_k and the number of parameters has been reduced by a factor of N (since for each k , only one function Φ_k is involved).

In the following we study the lowest exciton state, which for $V < 0$ is the lowest eigenfunction³ for $k = 0$. Hence, the wavefunction of interest has the form

$$\Psi = \frac{1}{\sqrt{N}} \sum_n |n \rangle G^n \Phi \quad (24.66)$$

and can be chosen real valued.

³This is the case of the so called J-aggregates [338] for which the lowest exciton state is strongly allowed.

24.2.1 Molecular Dimer

To begin with, let us consider a dimer ($N = 2$) consisting of two identical molecules in a symmetric arrangement. The model Hamiltonian reads in matrix form

$$H = -\frac{1}{2} \frac{\partial^2}{\partial q_1^2} - \frac{1}{2} \frac{\partial^2}{\partial q_2^2} + \begin{bmatrix} \frac{1}{2}(q_1 + \lambda)^2 + \frac{1}{2}q^2 & V \\ V & \frac{1}{2}q_1^2 + \frac{1}{2}(q_2 + \lambda)^2 \end{bmatrix} \quad (24.67)$$

and can be considerably simplified by introducing delocalized vibrations

$$q_{\pm} = \frac{q_1 \pm q_2}{\sqrt{2}} \quad (24.68)$$

which separates the symmetric mode q_+

$$H = \left(-\frac{1}{2} \frac{\partial^2}{\partial q_+^2} + \frac{1}{2} \left(q_+ + \frac{\lambda}{\sqrt{2}} \right)^2 \right) - \frac{1}{2} \frac{\partial^2}{\partial q_-^2} + \begin{bmatrix} \frac{1}{2} \left(q_- + \frac{\lambda}{\sqrt{2}} \right)^2 & V \\ V & \frac{1}{2} \left(q_- - \frac{\lambda}{\sqrt{2}} \right)^2 \end{bmatrix}. \quad (24.69)$$

The lowest eigenfunction of the symmetric oscillation is

$$\Phi_{0+} = \pi^{-1/4} \exp \left\{ -\frac{1}{2} \left(q_+ + \frac{\lambda}{\sqrt{2}} \right)^2 \right\} \quad (24.70)$$

with the eigenvalue (the zero point energy)

$$E_{0+} = \frac{1}{2}. \quad (24.71)$$

Hence, for the dimer we may consider a simplified Hamiltonian with only one vibration

$$H = \frac{1}{2} - \frac{1}{2} \frac{\partial^2}{\partial q^2} + \begin{bmatrix} \frac{1}{2} \left(q + \frac{\lambda}{\sqrt{2}} \right)^2 & V \\ V & \frac{1}{2} \left(q - \frac{\lambda}{\sqrt{2}} \right)^2 \end{bmatrix}. \quad (24.72)$$

According to (24.66) the $k = 0$ eigenstates have the form

$$\Psi = \frac{1}{\sqrt{2}} \Phi|1\rangle + \frac{1}{\sqrt{2}} G \Phi|2\rangle = \frac{1}{\sqrt{2}} \Phi(q)|1\rangle + \frac{1}{\sqrt{2}} \Phi(-q)|2\rangle. \quad (24.73)$$

For the dimer problem, the eigenstates can be calculated numerically by diagonalization of the Hamiltonian equation (24.72) in the basis of harmonic oscillator states [340].

Dressed Exciton

The simplest trial function which is well known as “dressed exciton” or “mean field” ansatz [341, 342], uses a Gaussian representing the groundstate of a displaced (and possibly distorted) harmonic oscillator

$$\Phi = \left(\frac{2\kappa}{\pi}\right)^{1/4} e^{-\kappa(q_+ + \alpha)^2} \quad G\Phi = \left(\frac{2\kappa}{\pi}\right)^{1/4} e^{-\kappa(q_+ - \alpha)^2} \quad (24.74)$$

with the energy expectation value

$$E_{MF}(\kappa, \lambda) = \langle \Psi H \Psi \rangle = \frac{1}{2} + \left(\frac{1}{8\kappa} + \frac{\kappa}{2}\right) + \frac{1}{2}\left(\alpha - \frac{\lambda}{\sqrt{2}}\right)^2 + V e^{-2\kappa\alpha^2} \quad (24.75)$$

for which the first and second derivatives are easily found

$$\frac{\partial E_{MF}}{\partial \alpha} = \alpha - \frac{\lambda}{\sqrt{2}} - 4V\alpha\kappa e^{-2\kappa\alpha^2} \quad (24.76)$$

$$\frac{\partial E_{MF}}{\partial \kappa} = \frac{1}{2} - \frac{1}{8\kappa^2} - 2V\alpha^2 e^{-2\kappa\alpha^2} \quad (24.77)$$

$$\frac{\partial^2 E_{MF}}{\partial \alpha^2} = 1 + 4V\kappa e^{-2\kappa\alpha^2} [4\kappa\alpha^2 - 1] \quad (24.78)$$

$$\frac{\partial^2 E_{MF}}{\partial \kappa^2} = \frac{1}{4\kappa^3} + 4V\alpha^4 e^{-2\kappa\alpha^2} \quad (24.79)$$

$$\frac{\partial^2 E_{MF}}{\partial \kappa \partial \alpha} = 4V\alpha e^{-2\kappa\alpha^2} [2\kappa\alpha^2 - 1]. \quad (24.80)$$

In the limit of vanishing “dressed” coupling $V e^{-2\kappa\alpha^2} \approx 0$, corresponding to the so called self trapped state, the lowest energy is found for $\alpha = \lambda/\sqrt{2}$, $\kappa = 1/2$

$$\min E_{MF}(V e^{-2\kappa\alpha^2} \rightarrow 0) = 1 \quad (24.81)$$

which is the zero point energy of the two dimer modes. In the limit of vanishing exciton-phonon coupling $\lambda = 0$ (the fully delocalized state) the energy is minimized for $\alpha = 0$, $\kappa = 1/2$

$$\min E_{MF}(\lambda \rightarrow 0) = V + 1. \quad (24.82)$$

For the general case we apply the Newton-Raphson method (p. 124) to locate the minimum. It is quite important to use a reasonable starting point to ensure conver-

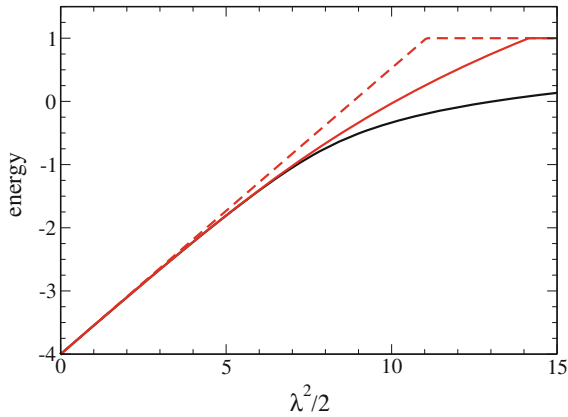


Fig. 24.15 (Variational solutions for the dimer) The lowest excitation energy of the dimer Hamiltonian is shown as a function of the reorganization energy $\lambda^2/2$. The mean field ansatz (*red curves*) predicts a sharp transition to the self-trapped state and deviates largely for $\lambda^2/2 > 5$. Variation of the exponent κ improves the agreement in the transition region considerably (*full red curve*) as compared to the standard treatment with fixed $\kappa = 1/2$ (*dashed red curve*). The *black curve* shows the numerically exact solution for comparison

gence to the lowest energy.⁴ In Problem 24.4, we search for an approximate minimum on a coarse grid first. Figure 24.15 shows the calculated energy minimum for strong excitonic coupling $V = -5$ as a function of λ^2 . For small values of the exciton-phonon coupling, the numerically exact values are reproduced quite closely. For larger values the mean field ansatz predicts a rapid transition to a so called self-trapped state [343] with $\alpha = \lambda/\sqrt{2}$ and a very small Franck-Condon factor $F = \exp(-2\kappa\alpha^2) \approx 0$ (Figs. 24.16, 24.17). In this region, the deviation from the numerical exact result is appreciable, especially if only α is varied and $\kappa = 1/2$ kept fixed.

Solitonic Solution

In the region of large exciton-phonon coupling a simple ansatz similar to Davydov's soliton [344] is quite successful (Fig. 24.18) which breaks the symmetry of the system and uses a trial function

$$\Psi_{sol} = (\varphi_1|1\rangle + \varphi_2|2\rangle)\Phi_{\alpha_1, \alpha_2}(q_1, q_2) \quad (24.83)$$

with two mixing amplitudes with the constraint

$$\varphi_1^2 + \varphi_2^2 = 1 \quad (24.84)$$

⁴In the transition region, the energy may converge to an unstable state, depending on the starting point.

Fig. 24.16 (Optimized parameters of the mean field ansatz) The optimized parameters for $V = -5$ show a sharp transition to the self trapped state. *Full curves* optimization of α and κ . *Dashed curves* optimization of α for fixed $\kappa = 1/2$

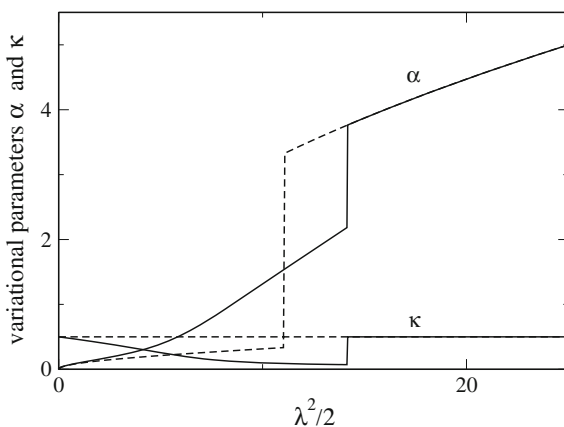


Fig. 24.17 (Franck-Condon factor of the mean field ansatz) The transition to the self trapped state shows also up in the Franck-Condon factor $F = \exp\{-2\kappa\alpha^2\}$ which is shown in a semi-logarithmic plot. *Full curve* optimization of α and κ . *Dashed curve* optimization of α for fixed $\kappa = 1/2$. The *dotted curve* shows the numerically exact result for comparison

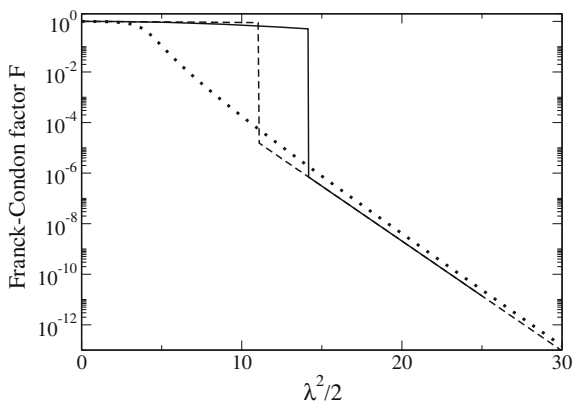
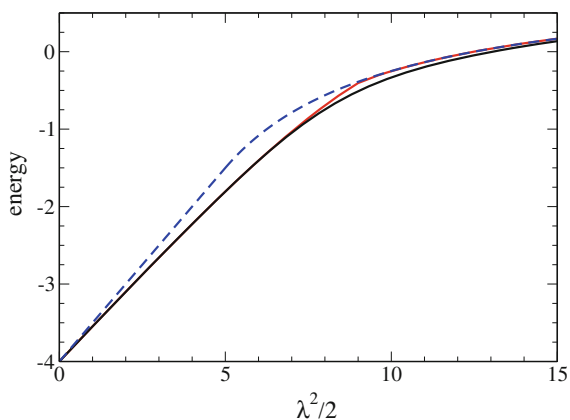


Fig. 24.18 (Variational solutions for the dimer) The soliton approach (*dashed blue curve*) works quite well for large but also for very weak exciton-phonon coupling. The delocalized soliton interpolates between mean field and soliton results and describes the transition quite well (*red curve*). The *black curve* shows the numerically exact solution for comparison



and the same vibrational function for both states (in the self trapped region distortion of the oscillator is not important)

$$\Phi_{\alpha_1, \alpha_2}(q_1, q_2) = \frac{1}{\sqrt{\pi}} e^{-(q_1 + \alpha_1)^2/2} e^{-(q_2 + \alpha_2)^2/2}. \quad (24.85)$$

The energy expectation value is

$$\begin{aligned} E_{sol}(\varphi_1, \varphi_2, \alpha_1, \alpha_2) &= \langle \Psi H \Psi \rangle \\ &= \varphi_1^2 \left[1 + \frac{(\alpha_1 - \lambda)^2}{2} + \frac{\alpha_2^2}{2} \right] + \varphi_2^2 \left[1 + \frac{(\alpha_2 - \lambda)^2}{2} + \frac{\alpha_1^2}{2} \right] + 2V\varphi_1\varphi_2 \\ &= 1 + \frac{1}{2}(\alpha_1 - \varphi_1^2\lambda)^2 + \frac{1}{2}(\alpha_2 - \varphi_2^2\lambda)^2 + \lambda^2\varphi_1^2\varphi_2^2 + 2V\varphi_1\varphi_2 \end{aligned} \quad (24.86)$$

and for the optimized values

$$\alpha_i^o = \varphi_i^2\lambda \quad (24.87)$$

it becomes

$$E_{sol}(\varphi_1, \varphi_2, \alpha_1^o, \alpha_2^o) = 1 + \lambda^2\varphi_1^2\varphi_2^2 + 2V\varphi_1\varphi_2 = 1 + \frac{\lambda^2}{4} \left(2\varphi_1\varphi_2 + \frac{2V}{\lambda^2} \right)^2 - \frac{V^2}{\lambda^2}. \quad (24.88)$$

Alternatively, using symmetrized coordinates we obtain

$$E_{sol}(\varphi_1, \varphi_2, \alpha_+, \alpha_-) = 1 + \frac{1}{2} \left(\alpha_+ - \frac{\lambda}{\sqrt{2}} \right)^2 + \frac{1}{2} \left(\alpha_- - \frac{\lambda}{\sqrt{2}} (\varphi_1^2 - \varphi_2^2) \right)^2 + \lambda^2\varphi_1^2\varphi_2^2 + 2V\varphi_1\varphi_2 \quad (24.89)$$

and optimum values

$$\alpha_+^o = \frac{\lambda}{\sqrt{2}} \quad (24.90)$$

$$\alpha_-^o = \frac{\lambda}{\sqrt{2}} (\varphi_1^2 - \varphi_2^2). \quad (24.91)$$

Since $|2\varphi_1\varphi_2| \leq 1$, the minimum for large exciton-phonon coupling is at the bottom of the parabola

$$\min E_{sol} = 1 - \frac{V^2}{\lambda^2} \quad \text{for } |V| < \lambda^2/2 \quad (24.92)$$

whereas in the opposite case it is found for $2\varphi_1\varphi_2 = 1$ (V is assumed to be negative)

$$\min E_{sol} = 1 + V + \frac{\lambda^2}{4} \quad \text{for } |V| > \lambda^2/2. \quad (24.93)$$

The transition between the two regions is continuous with

$$\min E_{sol} = 1 + \frac{V}{2} \quad \text{for } |V| = \lambda^2/2. \quad (24.94)$$

Delocalized Soliton Ansatz

Mean field and soliton ansatz can be combined by delocalizing the solitonic wave function [345]. The energies of the trial function

$$\Psi_{sol} = (\varphi_1|1 \rangle + \varphi_2|2 \rangle)\Phi \quad (24.95)$$

and its mirror image

$$\Psi'_{sol} = (\varphi_2|1 \rangle + \varphi_1|2 \rangle)G\Phi \quad (24.96)$$

are degenerate. Hence delocalization of the trial function

$$\Psi_{delsol} = |1 \rangle [\varphi_1\Phi + \varphi_2G\Phi] + |2 \rangle [\varphi_2\Phi + \varphi_1G\Phi] \quad (24.97)$$

is expected to lower the energy further and ensures the proper form of (24.73). Its norm is

$$\langle \Psi_{delsol} | \Psi_{delsol} \rangle = 2(1 + 2\varphi_1\varphi_2F) \quad (24.98)$$

with the Franck-Condon factor

$$F = \langle \Phi | G | \Phi \rangle = e^{-\kappa(\alpha_1 - \alpha_2)^2} = e^{-2\kappa\alpha^2}. \quad (24.99)$$

The expectation value of the Hamiltonian simplifies due to symmetry

$$\begin{aligned} \langle \Psi_{delsol} | H | \Psi_{delsol} \rangle &= 2\varphi_1^2 \langle \Phi | H_1 | \Phi \rangle + 2\varphi_2^2 \langle \Phi | H_2 | \Phi \rangle + 4\varphi_1\varphi_2 \langle \Phi | H_1 G | \Phi \rangle \\ &+ 2V [F + 2\varphi_1\varphi_2]. \end{aligned} \quad (24.100)$$

Finally, varying only the antisymmetric mode, the energy is

$$E_{delsol} = \frac{\kappa}{2} + \frac{1}{8\kappa} + \frac{\lambda^2}{2} + \frac{\frac{\alpha_-^2}{2} - (\varphi_1^2 - \varphi_2^2)\alpha_- \lambda + 2\varphi_1\varphi_2 [-2F\kappa^2\alpha_-^2 + V] + VF}{1 + 2\varphi_1\varphi_2F}. \quad (24.101)$$

In Problem 24.5 we locate the minimum energy with the steepest descent (6.2.5) or the conjugate gradient (6.2.5) method

24.2.2 Larger Aggregates

The variational methods for the dimer can be generalized for larger systems [345]. The mean field ansatz for the lowest $k = 0$ state becomes

$$\Psi_{MF} = \frac{1}{\sqrt{N}} \sum_n |n\rangle G^n \Phi \quad (24.102)$$

with

$$\Phi = \prod_{n=1}^N \pi^{-1/4} e^{-(q_n + \alpha_n)^2/2}. \quad (24.103)$$

The energy is

$$\begin{aligned} E_{MF} &= \frac{1}{N} \sum_n \langle \Phi G^{-n} H_n G^n \Phi \rangle + V \langle \Phi G \Phi \rangle + V \langle \Phi G^{-1} \rangle \\ &= \langle \Phi H_0 \Phi \rangle + 2VF \\ &= \frac{N}{2} + \frac{\lambda^2}{2} - \alpha_0 \lambda + \sum_n \frac{\alpha_n^2}{2} + 2VF \end{aligned} \quad (24.104)$$

and its gradient

$$\frac{\partial E_{MF}}{\partial \alpha_n} = -\lambda \delta_{n,0} + \alpha_n - VF(2\alpha_n - \alpha_{n+1} - \alpha_{n-1}).$$

In Problem 24.5 we locate the minimum energy with the steepest descent (6.2.5) or the conjugate gradient (6.2.5) method. As for the dimer, the mean field method shows a rapid transition to the self-trapped state. The starting point is quite important as in the vicinity of the transition the gradient based methods eventually converge to a metastable state (Fig. 24.19).

The soliton wavefunction (corresponding to Davydov's D1 soliton) for the aggregate is

$$\Psi_{sol} = \sum_n \varphi_n |n\rangle \Phi \quad (24.105)$$

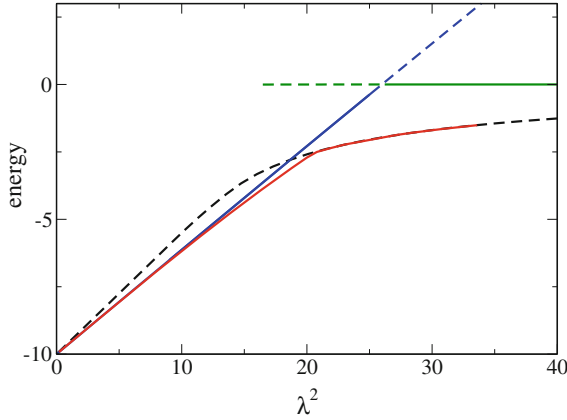


Fig. 24.19 (Variational solutions for a 10-mer) The lowest energy of a periodic 10-mer is calculated for $V = -5$ (see Problem 24.5). The mean field wavefunction gives (green and blue curves) reasonable values for small values of λ^2 and predicts a rapid transition to the self trapped state. Approaching the transition from below or above the calculation may end up in a metastable state (dashed green and blue curves). The solitonic wavefunction (dashed black curve) provides lower energies at larger values of λ^2 and a much smoother transition to the self trapped state. The delocalized soliton (red curve) gives the lowest energy at all values of λ^2 . The zero point energy has been subtracted

with the constraint

$$\sum_n \varphi_n^2 = 1 \tag{24.106}$$

where Φ is given by (24.103). The energy is

$$\begin{aligned} E_{sol} &= \langle \Psi_{sol} | H | \Psi_{sol} \rangle = \sum_n \varphi_n^2 \langle \Phi | H_n | \Phi \rangle + V \sum_n (\varphi_n \varphi_{n+1} + \varphi_n \varphi_{n-1}) \\ &= \frac{N}{2} + \sum_n \frac{\alpha_n^2}{2} + \frac{\lambda^2}{2} - \lambda \sum_n \varphi_n^2 \alpha_n + V \sum_n (\varphi_n \varphi_{n+1} + \varphi_n \varphi_{n-1}) \\ &= \frac{N}{2} + \sum_n \frac{(\alpha_n - \lambda \varphi_n^2)^2}{2} + \frac{\lambda^2}{2} \left(1 - \sum_n \varphi_n^4 \right) + V \sum_n (\varphi_n \varphi_{n+1} + \varphi_n \varphi_{n-1}) \end{aligned} \tag{24.107}$$

with the optimum displacements

$$\alpha_n^o = \lambda \varphi_n^2. \tag{24.108}$$

The energy functional becomes

$$E_{sol}(\varphi_n, \alpha_n^0) = \frac{N}{2} + \frac{\lambda^2}{2} \left(1 - \sum_n \varphi_n^4 \right) + 2V \sum_n \varphi_n \varphi_{n+1} \quad (24.109)$$

and its gradient

$$\frac{\partial E_{sol}}{\partial \varphi_n} = -2\lambda^2 \varphi_n^3 + 2V(\varphi_{n-1} + \varphi_{n+1}). \quad (24.110)$$

In Problem 24.5 we locate the minimum energy by varying the φ_n under the constraint (24.106). At larger exciton-phonon coupling, the energy of the soliton wavefunction is much lower in energy than the mean field result and the transition to the self-trapped state is smoother. At small exciton-phonon coupling, the mean field ansatz is lower in energy (Fig. 24.19).

Similar to the dimer case, the solitonic wavefunction can be delocalized by combining the N degenerate mirror images

$$\sum_n \varphi_n |n + m\rangle > G^m \Phi \quad m = 1 \cdots N \quad (24.111)$$

into the trial function

$$\begin{aligned} \Psi_{delsol} &= \frac{1}{\sqrt{N}} \sum_m e^{ikm} \sum_n \varphi_n |n + m\rangle > G^m \Phi \\ &= \frac{1}{\sqrt{N}} \sum_{nn'} e^{ik(n'-n)} \varphi_n |n'\rangle > G^{n'-n} \Phi = \frac{1}{\sqrt{N}} \sum_{n'} e^{ikn'} |n'\rangle > G^{n'} \sum_n e^{-ikn} \varphi_n G^{-n} \Phi. \end{aligned} \quad (24.112)$$

From the squared norm

$$\langle \Psi_{delsol} | \Psi_{delsol} \rangle = \sum_{nn'} \varphi_n \varphi_{n'} \langle \Phi G^{n-n'} \Phi \rangle = \sum_{nn'} \varphi_n \varphi_{n'} F_{n-n'} \quad (24.113)$$

and the expectation value

$$\begin{aligned} \langle \Psi_{delsol} | H | \Psi_{delsol} \rangle &= \frac{1}{N} \sum_{m,n,m',n'} \langle \Phi G^{-m} \langle n + m | \varphi_n H \varphi_{n'} | m' + n' \rangle G^{m'} \Phi \rangle \\ &= \frac{1}{N} \sum_{m,n,m',n'} \langle \Phi G^{-m} \varphi_n H_{n+m} \varphi_{n'} G^{m+n-n'} \Phi \rangle \\ &+ \frac{1}{N} \sum_{m,n,m',n'} V \langle \Phi G^{-m} \varphi_n \varphi_{n'} G^{m+n-n'+1} \Phi \rangle \end{aligned}$$

$$\begin{aligned}
& + \frac{1}{N} \sum_{m,n,n'} V \langle \Phi G^{-m} \varphi_n \varphi_{n'} G^{m+n-n'-1} \Phi \rangle \\
& = \sum_{n,n'} \varphi_n \varphi_{n'} \langle \Phi G^n H_0 G^{-n'} \Phi \rangle \\
& + V \sum_{n,n'} \varphi_n \varphi_{n'} \langle \Phi G^{n-n'+1} \Phi \rangle + V \sum_{n,n'} \varphi_n \varphi_{n'} \langle \Phi G^{n-n'-1} \Phi \rangle
\end{aligned} \tag{24.114}$$

we obtain the energy of the $k = 0$ state

$$\begin{aligned}
E_{delsol} & = \frac{N}{2} + \frac{\lambda^2}{2} \\
& + \left(\sum_{nn'} \varphi_n \varphi_{n'} \frac{1}{2} \left[-\lambda(\alpha_{n'} + \alpha_{n'-n}) + \sum_m \alpha_m \alpha_{m+n'-n} \right] F_{n'-n} \right. \\
& \left. + V \sum_{nn'} \varphi_n \varphi_{n'} (F_{n'-n+1} + F_{n'-n-1}) \right) \left(\sum_{nn'} \varphi_n \varphi_{n'} F_{n-n'} \right)^{-1}
\end{aligned} \tag{24.115}$$

with the Franck-Condon factors

$$F_k = \langle \Phi G^k \Phi \rangle = e^{-\sum_m (\alpha_m - \alpha_{m+k})^2 / 4} = e^{-\sum_m (\alpha_m^2 - \alpha_m \alpha_{m+k}) / 2}. \tag{24.116}$$

The results for longer aggregates are qualitatively similar to the dimer. The delocalized soliton interpolates between mean field and soliton wave functions and shows a smooth transition (Fig. 24.19).

Problems

In the first three computer experiments, we use the variational quantum Monte Carlo method to calculate the groundstate energy. The Metropolis algorithm with N_w walkers is used to evaluate the integral

$$E(\kappa, R) = \frac{\langle \psi_\kappa H \psi_\kappa \rangle}{\langle \psi_\kappa \psi_\kappa \rangle} = \int d^3 r \frac{|\psi_\kappa(\mathbf{r})|^2}{\int |\psi_\kappa(\mathbf{r}')|^2 d^3 r'} E_{loc}(\mathbf{r}).$$

Adjust the maximum trial step to obtain an acceptance ration of about 1 and study the influence of the number of walkers on the statistical error.

Problem 24.1

Optimize the effective nuclear charge κ for the hydrogen molecular ion H_2^+ as a function of R and determine the equilibrium bond length. The trial function has the form

$$\psi_{\text{trial}} = \sqrt{\frac{\kappa^3}{\pi}} e^{-\kappa r_a} + \sqrt{\frac{\kappa^3}{\pi}} e^{-\kappa r_b}.$$

Problem 24.2

For the Helium atom we use a trial wavefunction of the Slater-Jastrow type

$$\psi_{\text{trial}} = e^{-\kappa r_1} e^{-\kappa r_2} e^{\alpha r_{12}/(1+\beta r_{12})} \frac{1}{\sqrt{2}} (\uparrow(1) \downarrow(2) - \uparrow(2) \downarrow(1))$$

to find the optimum parameters α , β , κ .

Problem 24.3

In this computer experiment we study the hydrogen molecule H_2 . The trial function has the form

$$\psi_{\text{trial}} = \{C [e^{-\kappa r_{1a} - \kappa r_{2b}} + e^{-\kappa r_{1b} - \kappa r_{2a}}] + (1 - C) [e^{-\kappa r_{1a} - \kappa r_{2a}} + e^{-\kappa r_{1b} - \kappa r_{2b}}]\} \\ \times \exp\left\{\frac{\alpha r_{12}}{1 + \beta r_{12}}\right\}.$$

Optimize the parameters κ , β , C as a function of R and determine the equilibrium bond length.

Problem 24.4

In this computer experiment we simulate excitons in a molecular dimer coupled to molecular vibrations. The energy of the lowest exciton state is calculated with the dressed exciton trial function including a frequency change of the vibration

$$\psi_{\text{trial}} = \frac{1}{\sqrt{2}} |1\rangle > \left(\frac{2\kappa}{\pi}\right)^{1/4} e^{-\kappa(q_+ + \alpha)^2} + \frac{1}{\sqrt{2}} |2\rangle > \left(\frac{2\kappa}{\pi}\right)^{1/4} e^{-\kappa(q_- - \alpha)^2}.$$

The parameters κ , α are optimized with the Newton-Raphson method. Vary the exciton coupling V and the reorganization energy $\lambda^2/2$ and compare with the numerically exact values.

Problem 24.5

In this computer experiment we simulate excitons in a molecular aggregate coupled to molecular vibrations. The energy of the lowest exciton state is calculated with different kinds of trial functions

- the dressed exciton

$$\Psi_{MF} = \frac{1}{\sqrt{N}} \sum_n |n\rangle G^n \prod_{n=1}^N \pi^{-1/4} e^{-(q_n + \alpha_n)^2/2}$$

- the soliton

$$\Psi_{sol} = \sum_n \varphi_n |n\rangle \prod_{n=1}^N \pi^{-1/4} e^{-(q_n + \alpha_n)^2/2}$$

- the delocalized soliton

$$\Psi_{delsol} = \frac{1}{\sqrt{N}} \sum_m \sum_n \varphi_n |n+m\rangle G^m \prod_{n=1}^N \pi^{-1/4} e^{-(q_n + \alpha_n)^2/2}.$$

The system size can be varied from a dimer (N=2) up to chains of 100 molecules. The N equilibrium shifts α_n and the N excitonic amplitudes φ_n are optimized with the methods of steepest descent or conjugate gradients. The optimized parameters are shown graphically. Vary the exciton coupling V and the reorganization energy $\lambda^2/2$ and study the transition from a delocalized to a localized state. Compare the different trial functions.